Title

Trans-Ocular Electric Current In Vivo Enhances AAV-Mediated Retinal Transduction in Large Animal Eye After Intravitreal Vector Administration

Journal

Translational Vision Science & Technology, 9(7)

ISSN

2164-2591

Authors

Song, Hongman
Zeng, Yong
Pasha, Pran Babu Sardar
et al.

Publication Date

2020-06-24

DOI

10.1167/tvst.9.7.28

Peer reviewed

tvst

Article

Trans-Ocular Electric Current In Vivo Enhances AAV-Mediated Retinal Transduction in Large Animal Eye After Intravitreal Vector Administration

Hongman Song[1,2], Yong Zeng[1,2], Sheik Pran Babu Sardar Pasha[3], Ronald A. Bush[1,2], Camasamudram Vijayasarathy[1,2], Haohua Qian[2], Lisa Wei[2], Henry E. Wiley[2], Zhijian Wu[2], and Paul A. Sieving[1–3]

[1] Section for Translational Research on Retinal and Macular Degeneration, National Institute on Deafness and Other Communication Disorders, Bethesda, MD, USA
[2] National Eye Institute, National Institutes of Health, Bethesda, MD, USA
[3] Department of Ophthalmology, School of Medicine, University of California at Davis, Sacramento, CA, USA

Correspondence: Paul A. Sieving, Center for Ocular Regenerative Therapy; UC Davis Eye Center; 4860 Y Street, Suite 2400; Sacramento, CA 95817, USA. e-mail: pasieving@UCDavis.edu

Received: December 2, 2019
Accepted: May 6, 2020
Published: June 24, 2020

Keywords: AAV vector; electric current; gene delivery and expression in the retina; intravitreal administration; large-animal models

Citation: Song H, Zeng Y, Sardar Pasha SPB, Bush RA, Vijayasarathy C, Qian H, Wei L, Wiley HE, Wu Z, Sieving PA. Trans-ocular electric current in vivo enhances AAV-Mediated retinal transduction in large animal eye after intravitreal vector administration. Trans Vis Sci Tech. 2020;9(7):28, https://doi.org/10.1167/tvst.9.7.28

Purpose: Electric micro-current has been shown to enhance penetration and transduction of adeno-associated viral (AAV) vectors in mouse retina after intravitreal administration. We termed this: "electric-current vector mobility (ECVM)." The present study considered whether ECVM could augment retinal transduction efficiency of intravitreal AAV8-CMV-EGFP in normal rabbit and nonhuman primate (NHP) macaque. Potential mechanisms underlying enhanced retinal transduction by ECVM were also studied.

Methods: We applied an electric micro-current across the intact eye of normal rabbit and monkey in vivo for a brief period immediately after intravitreal injection of AAV8-CMV-EGFP. Retinal GFP expression was evaluated by fundus imaging in vivo. Retinal immunohistochemistry was performed to assess the distribution of retinal cells transduced by the AAV8-EGFP. Basic fibroblast growth factor (bFGF) was analyzed by quantitative RT-polymerase chain reaction (PCR). Müller glial reactivity and inner limiting membrane (ILM) were examined by the glial fibrillary acidic protein (GFAP) and vimentin staining in mouse retina, respectively.

Results: ECVM significantly increased the efficiency of AAV reaching and transducing the rabbit retina following intravitreal injection, with gene expression in inner nuclear layer, ganglion cells, and Müller cells. Similar trend of improvement was observed in the ECVM-treated monkey eye. The electric micro-current upregulated bFGF expression in Müller cells and vimentin showed ILM structural changes in mouse retina.

Conclusions: ECVM promotes the transduction efficiency of AAV8-CMV-GFP in normal rabbit and monkey retinas following intravitreal injection.

Translational Relevance: This work has potential translational relevance to human ocular gene therapy by increasing retinal expression of therapeutic vectors given by intravitreal administration.

Introduction

Recombinant adeno-associated viral (AAV) vectors have become useful for gene delivery. With increased AAV-based ocular gene therapies reaching clinical trials, approaches and strategies for high efficiency of AAV gene transfer in the eyes are urgently demanded.[1] For clinical drug delivery to the retina, intravitreal (IVT) administration is preferable to subretinal injection of vector because it is surgically less invasive and would reach more of the retina.[2] By the IVT delivery

approach, however, most conventional, nonmodified AAV serotypes show limited gene transduction in the retina.[3–8]

A previous proof-of-concept study in mice demonstrated that a weak transocular electric current enhanced penetration of AAV vectors across the inner limiting membrane (ILM) after intravitreal vector administration.[9] We termed this: "electric-current vector mobility (ECVM)." These encouraging results in mice led us to test this approach in large-animal models, the rabbit and monkey, for retinal translational studies. Compared with the mouse eye, the rabbit and monkey eyes are closer in size and structure to humans, including relative size of the lens, vitreous, and retinal surface area.[10–16] Similarities in vitreous characteristics and the retinal structure indicate that the monkey eye is preferable to the mouse or rabbit eye. As the vitreous, ILM and laminated retina are reported to be major barriers to AAV-mediated retinal transduction,[17,18] we explored whether ECVM could augment retinal transduction in the larger eye.

The present study was designed to evaluate the extension of this experimental concept to rabbit and nonhuman primate (NHP) macaque monkey. We tested AAV8 vector, which is in current use, including in human clinical trials (ClinicalTrials.gov NCT02317887). Pre-existing immunity to the AAV capsid could limit the vector expression after intravitreal administration.[19,20] Compared with other commonly used AAVs, such as AAV2, neutralizing antibodies against AAV8 in the human vitreous and serum are reported to be less prevalent.[21,22] Thus, we selected AAV8 vector to reduce the probability of developing anti-AAV antibody-mediated immune response in the AAV-injected eye, increasing the chance of gene therapeutic success. We asked whether transocular ECVM can augment retinal transduction efficiency of AAV8-CMV-EGFP administrated intravitreally in normal rabbit and monkey eyes. We also attempted to address possible mechanisms underlying enhanced AAV-mediated retinal transduction by transocular electric current.

Methods

Animals

Regular New Zealand White male rabbits 6 to 8 months old (Covance, Princeton, NJ), a rhesus macaque (age: approximately 5 years old, India origin, inbred, and raised "in-house") and wild-type C57BL/6J mice 8 to 12 weeks old (Jackson Laboratory, Bar Harbor, ME) were used in the studies. All animals were housed on a 12 hour/12 hour light/dark cycle. Experimental protocols were approved by the National Institutes of Health (NIH) Animal Care and Use Committee and adhered to the ARVO Statement for the Use of Animals in Ophthalmic and Vision Research.

Anesthesia was performed with intramuscular (IM) ketamine (40 mg/kg) and xylazine (3 mg/kg) for the rabbit or IM ketamine (7 mg/kg) and dexmedetomidine (40 mcg/kg) for the monkey. Pupils were dilated with topical ocular 1% tropicamide (Alcon Laboratories, Inc.) and 2.5% phenylephrine hydrochloride (Bausch & Lomb, Inc.) after topical 0.5% proparacaine was applied to the eye. For mouse experiments, anesthesia was performed with intraperitoneal (IP) ketamine (92.6 mg/kg)/xylazine (5.6 mg/kg) solution; and pupils were dilated with topical ocular 0.5% tropicamide and 0.5% phenylephrine hydrochloride after topical 0.5% tetracaine was applied to the eye.

Adeno-Associated Virus Serotype 8 vector

The AAV8-CMV-EGFP vector has a cytomegalovirus (CMV) promoter, a chimeric CMV/human β-globin intron, the enhanced green fluorescent protein (EGFP) gene, and a human β-globin polyadenylation (PolyA) site. Recombinant AAV was produced by the triple transfection method and purified by polyethylene glycol precipitation followed by cesium chloride density-gradient fractionation, as previously described.[23] The purified AAV vectors were formulated in 10 mM Tris–HCl, 180 mM NaCl pH 7.4, and 0.001% Pluronic F-68 pH 7.4, and stored at -80°C. Quantification of vectors was done by real time polymerase chain reaction (PCR) using linearized plasmid standards.

Intravitreal Injection and Ocular ECVM Application

In rabbits, AAV8-CMV-EGFP vector dilutions 5×10^{11} vg/eye were administered by intravitreal injection, as described previously.[24] Briefly, rabbits were first anesthetized and pupils dilated. Then, 50 µl of viral vector was injected into the midvitreous through the pars plana approximately 2 mm posterior to the limbus in superotemporal quadrant using a $\frac{1}{2}$ cc U-100 insulin syringe with attached 28-gauge needle (Becton, Dickinson and Company, Franklin Lakes, NJ). For monkey eyes, the pupillary dilation was accomplished after the animal was anesthetized. AAV-CMV-EGFP vector (1×10^{12} vg/dose in 50 ul) was intravitreally injected into the eye using a 1 cc Tuberculin syringe

(EXELINT International, Co., Redondo Beach, CA) with 30-gauge 1-inch needle (Becton, Dickinson and Company) inserted through the pars plana approximately 2 mm posterior to the limbus in superotemporal quadrant. The injection was performed with direct visualization of the needle tip using an operating microscope (Zeiss, Jena, German) with coaxial illumination (Ngenuity; Alcon, Fort Worth, TX). Under direct visualization, the needle tip was slowly advanced to the desired location in the posterior vitreous cavity, and the vector fluid was ejected gently under manual control. Injected eyes then received ECVM application immediately (approximately 5 minutes) after injection. Injected eyes without electric current application served as controls. An antibiotic ophthalmic ointment of neomycin was applied to the eyes.

Transocular ECVM Application

For rabbits and monkeys, a Burian-Allen ERG electrode was placed on the center of cornea with a thin layer of GONAK Hypromellose immediately after intravitreal injection. A subdermal needle electrode was inserted subcutaneously behind the ipsilateral side of the head as the second electrode to complete the electrical circuit. DC current (800 to approximately 850 μA cornea-negative, monophasic, continuous) was applied for 20 minutes from a stimulus-isolator constant current power supply (A365; World Precision Instruments, Sarasota, FL).

Mice were treated with transocular ECVM (continuous direct current 10 μA/20 minutes, cornea-negative) as described previously by Song et al.[9] Briefly, a gold wire ring electrode was placed on the center of the cornea and a subdermal needle electrode was inserted subcutaneously on the forehead above the same eyelid as the second electrode to complete the electrical circuit.

GFP Expression by In Vivo Fundus Imaging

GFP expression was evaluated by fundus imaging in vivo. Fundus images were obtained using confocal scanning laser ophthalmoscopy (cSLO; Spectralis; Heidelberg Engineering, Franklin, MA). Animals were first anesthetized, and the pupils were dilated. The cornea was lubricated with Systane Ultra (Alcon, Fort Worth, TX). An eyelid speculum was inserted to keep the eye open during imaging. The fundi of animal eyes were viewed using a 55° wide-field lens in blue autofluorescence mode with a 488 nm laser to capture the high fluorescence region. To quantify and compare GFP expression in rabbit retina, we used an expression index defined as GFP positive area times GFP fluorescence intensity in the medullated retinal region, which was estimated from fundus photographs. Specifically, GFP pixel area and intensity were measured along the entire medullated regions in fundus micrographs using an intensity threshold method with ImageJ software (http://imagej.nih.gov/ij/), as previously described.[9] In brief, the analysis used photographs with the entire medullated regions around the optic disc. An intensity threshold was applied by ImageJ software to select GFP-positive areas from background signals. Then the software measured the GFP pixel area and intensity. A larger expression index indicates stronger GFP expression and/or larger AAV GFP-transduced retinal area.

Immunohistochemistry

Retinal immunohistochemistry was performed as described by Song et al.[25] Briefly, eyes were fixed, cryoprotected, embedded, and snap-frozen in Tissue-Tek O.C.T. compound (Sakura Finetek USA, Inc., Torrance, CA), and cryo-sectioned at 14-μm thickness. Cryo-sections were blocked in blocking buffer and incubated with anti-GFP (mouse, 1:1000;, Cell Signaling Technology, Danvers, MA), or Calbindin (mouse, 1:2000; Sigma-Aldrich, St. Louis, MO), or Parvalbumin (rabbit, 1:1000; Abcam, Cambridge, MA), or Brn3a (mouse, 1:100; EMD Millipore, Temecula, CA), or Glutamine synthetase (GS, mouse, 1:1000; EMD Millipore, Temecula, CA) primary antibodies overnight at 4°C, and then incubated with appropriate secondary antibodies either conjugated to Alexa Fluor 488 or Alexa Fluor 568 (1:1000; Invitrogen, Eugene, OR). Retinal nuclei were counterstained with DAPI and sections were mounted in Fluoro-Gel buffer (Electron Microscopy Sciences, Hatfield, PA) for imaging. The images were generated and analyzed by the Nikon C2 confocal microscope (Nikon, Tokyo, Japan) with NIS-elements AR software, and further edited using Adobe Photoshop CC (Adobe Systems Inc., San Jose, CA). The same imaging setting (without post-processing using Photoshop) was used only for comparison of retinal GFP expression between ECVM-treated and control groups (i.e. Figs. 2A, 2B, Figs. 3C, 3D, 3E, 3F).

Quantitative Analysis of Basic Fibroblast Growth Factor by RT-PCR

Mice were treated with transocular ECVM and untreated littermates served as controls. At either 1 hour or 24 hours after treatment, retinal tissues were collected for real-time quantitative RT-PCR (qRT-PCR) analysis. Total RNA was extracted using Trizol

reagent based miRNeasy Mini Kit (Qiagen, Germantown, MD) according to the manufacturer's instructions. The RT^2 Easy First Strand Kit (Qiagen) was used for first strand cDNA synthesis, including elimination of contaminating genomic DNA from RNA samples. About 2 µg of total RNA was used for cDNA synthesis with random hexamers following the manufacturer's protocol. These cDNA samples were used as templates for qPCR. Relative expression levels of basic fibroblast growth factor (bFGF) were quantified using TaqMan mRNA assays on the Quantstudio 7 Flex Real-Time PCR System with TaqMan probes (Thermo Fisher Scientific, Carlsbad, CA). Reactions were run in triplicate. The 18S rRNA was amplified as an endogenous control. The results were expressed as n-fold induction or inhibition in gene expression relative to endogenous control calculated using the $2^{-\Delta\Delta CT}$ method. The data was processed using QuantStudio 6 and 7 Flex Real-Time PCR System Software. Quantitative RT-PCR data are represented as a fold change in relative levels of bFGF expression compared to those in untreated WT control retinas (ECVM-treated retina/control retina).

Real-time RT–PCR primers/probes for mRNA expression analysis:

Gene Symbol	Source	Assay Type	Assay ID/Catalog No.
bFGF	Thermo Fisher Scientific	TaqMan	Mm01285715_m1
Rn 18S	Thermo Fisher Scientific	TaqMan	Mm04277571_s1

Glial Fibrillary Acidic Protein Expression on Mouse Retinal Cross Sections

Mice were treated with transocular ECVM. Untreated littermates served as controls. At 1 hour, 1 day, or 7 days after treatment, animals were euthanized. Retinal cryosections were obtained and then subjected to immunohistochemistry with anti-glial fibrillary acidic protein (GFAP) antibody (mouse, 1:1000; Sigma-Aldrich). The same imaging setting was used for analysis of all samples. Examination was done on three or four retinas for each time point.

Retinal Flat-Mount Preparation and Whole Mount Staining

Mice were treated with ECVM and untreated littermates were controls. At various time points (day 1, 2, 4, and 7) after ECVM treatment, animals were euthanized, and the eyes were enucleated and fixed in 4% PFA for 2 hours at room temperature. The retinal flat-mounts were prepared and immunostained, as per the previously published protocol.[26] Briefly, after removal of optic nerve, the anterior eye parts and lens were removed and the retina was carefully dissected from the retinal pigment epithelium (RPE)–choroid–sclera complex and transferred to a glass slide. Four radial incisions were made 2 mm apart from the site of the optic nerve with the microdissection scissors to allow the retina to lie flat for imaging. In some cases, to prevent curling of the retina, the edge of the quadrant was removed using the No. 11 scalpel blade. Retinal flat-mounts were fixed overnight at 4°C. After fixation, retinal flat-mounts were washed thrice in PBS and permeabilized for 2 hours in blocking buffer containing 0.5% Triton X-100 in 10% BSA in PBS. After incubation, retinal flat-mounts were co-stained for anti-GFAP antibody (mouse, 1:500; Sigma-Aldrich) and anti-vimentin antibody (rabbit, 1:500; Abcam) in flat-mount staining solution containing 0.5% Triton X-100 in 1% BSA in PBS and kept for 2 to 3 days at 4°C on a shaker. After the incubation, retinal flat-mounts were washed thrice in PBS for 15 minutes each and respective secondary antibodies at 1:500 dilution were added to each retina and incubated overnight at 4°C on a shaker protected from light. After staining, retinal flat-mounts were again washed in PBS. Finally, immunostained retinal flat-mounts were transferred to a glass slide and cover-slipped with Fluoro-Gel mounting solution (Electron Microscopy Sciences, Hatfield, PA) for imaging. The same imaging setting was used for analysis of all samples. Examination was done on six retinas for each time point.

Statistical Analysis

Quantitative data are presented as mean ± SEM. To compare means between two groups, we first did a D'Agostino & Pearson omnibus normality test in GraphPad Prism 6.07 for Windows (GraphPad Software; La Jolla, CA). For datasets that passed normality test, we used Student's *t*-test. If not, we used the Mann–Whitney *U* test.

Results

ECVM Enhances the Retinal Transduction of AAV8 Vectors in the Rabbit After Intravitreal Delivery

We evaluated whether ECVM would enhance the retinal transduction efficiency of AAV8-CMV-GFP when current was applied immediately after 5×10^{11} vector genomes (vg) were injected into the vitreous of the rabbit eye. Control eyes were injected with the GFP vector, but no current was applied. Retinal GFP

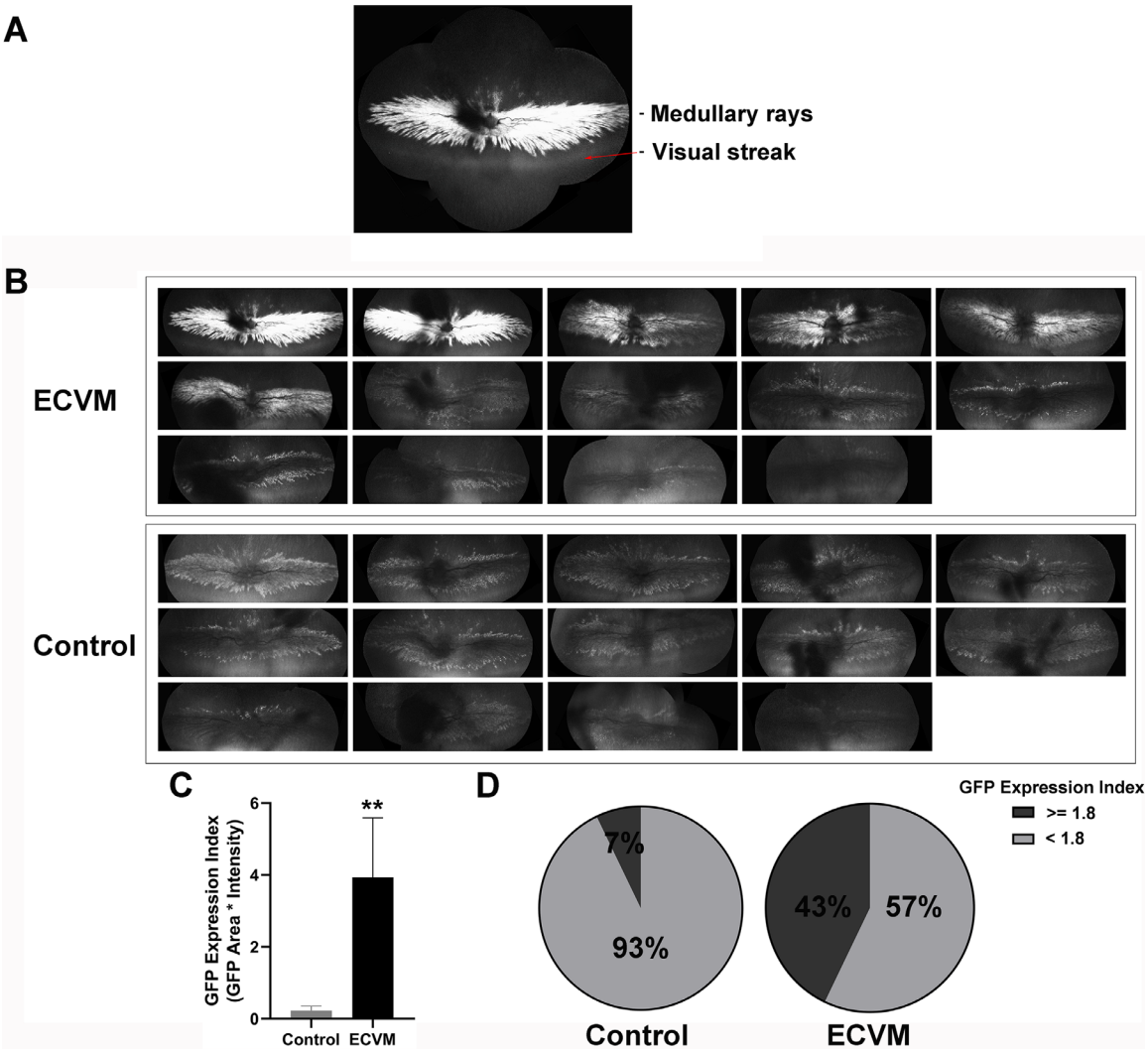

Figure 1. Electric-current vector mobility (ECVM) enhances AAV8-mediated gene transduction in rabbit retina. Normal rabbit eyes were treated with ECVM (continuous, cornea negative, direct current 800 μA/20 minutes) immediately after intravitreal injection of AAV8-CMV-EGFP at 5×10^{11} vg/eye. Vector-injected eyes without applying ECVM served as controls. Fundus images were taken 11 weeks post-injection (PI). (**A**) Representative in vivo fundus autofluorescence photograph of the rabbit retina shows the specialized regions of the retina, the medullary rays, and visual streak. (**B**) All eyes of ECVM treated (ECVM) and control groups (Control) are shown. (**C**) GFP expression index (GFP area * intensity) was represented as an average (mean ± SEM) for control ($n = 14$) and ECVM ($n = 14$) groups, respectively. ** $P = 0.0033$, Mann–Whitney *U* test. (**D**) Pie graphs show the probability of eyes with GFP expression index of 1.8 or larger and eyes with index less than 1.8 in control and ECVM-treated groups, respectively.

expression was monitored at 11 weeks post-injection (PI) by in vivo fundus autofluorescence imaging and immunohistochemistry.

The rabbit retina has myelinated nerve fibers radiating from the optical nerve head, termed the medullary rays (Fig. 1A). The fundus showed the majority of GFP signals in this area at 11 weeks after vector application (Fig. 1B). We used the extent of GFP expression in the medullated region to indicate relative efficiency of AAV vector transduction. The extent of GFP expression was represented as an expression index, which is defined as the GFP positive area times the GFP fluorescence intensity (GFP area * intensity; Fig. 1C). A larger expression index indicates stronger GFP expression and/or lager area of AAV GFP-transduced retina.

The mean GFP expression index (area * intensity) was significantly larger in eyes that were treated by the approach of ECVM (3.9; $n = 14$) than for the control group (0.2; $n = 14$; $P = 0.0033$; Mann–Whitney *U* test; see Fig. 1C). In the control eyes, 1 of the 14 (7%) had a visible but weak GFP signal across the medullary

rays, which had the highest GFP expression (expression index 1.8) in the control group (Figs. 1B, 1D, control). We chose this expression index 1.8 as the cutoff point. The majority of the control eyes showed little or no GFP expression, as 13 of the 14 (93%) control eyes had GFP expression index < 1.8 (see Fig. 1D). By comparison, 6 of the 14 eyes (43%) receiving ECVM had the larger expression index than 1.8 at the area of medullary rays (Figs. 1B, 1D, ECVM). These results indicate that transocular ECVM increased the efficiency of AAV vector reaching and transducing the rabbit retina following intravitreal injection.

We also evaluated the distribution of retinal cells transduced by the AAV-EGFP in ECVM-treated eyes. GFP was observed in several retinal layers, with the highest GFP intensities in the nerve fiber layer (i.e. the medullary rays; see Fig. 2B). GFP was also seen in cells in the inner nuclear layer (INL; e.g. Calbindin positive horizontal cells, and Parvalbumin positive horizontal and amacrine cells; Figs. 2C–2H) and ganglion cell layers (GCLs; Figs. 2I–2K). AAV transduction and expression were also observed in some Müller glial cells, including processes stretching across the thickness of outer nuclear layer (ONL) to the outer limiting membrane (OLM; Figs. 2L–2N). Occasionally, a few of the RPE cells were GFP positive (see Fig. 2E). Some retinal regions showed abundant spotty GFP signals in the inner plexiform layer (IPL; see Fig. 2B, 2E, 2H). By comparison, control sections from eyes that did not receive transocular current showed considerably less GFP expression and smaller extent of GFP signals across retina (see Fig. 2A).

ECVM Improves AAV8-Mediated Retinal Transduction From the Vitreous in the Nonhuman Primate Retina

We further evaluated the retinal transduction of AAV8-CMV-GFP vector in a rhesus monkey when ECVM was applied immediately after 1×10^{12} vg in 50 µl were injected into the vitreous of the eye. The GFP vector-injected contralateral eye without applying ECVM served as a control. Retinal GFP expression was monitored in vivo by fundus autofluorescence imaging. At 12 weeks after injection, autofluorescence imaging showed higher GFP signals in and around the foveal regions (Fig. 3B, yellow arrow) of ECVM-treated retina, compared with the control (Fig. 3A, yellow arrow).

The distribution of retinal cells transduced by the AAV8-EGFP in the foveal regions of ECVM-treated eyes showed GFP in all the retinal layers. GFP intensity was higher in the RGC, IPL, INL; and outer plexiform (OPL) layers and lowest in the ONL (see Fig. 3D, 3F). Control sections injected with GFP-vector but without current showed less GFP expression across the retina (see Fig. 3C, 3E).

Transocular Electric Current Upregulates bFGF and Changes Müller Glial Reactivity and ILM Structure

We explored the potential mechanisms underlying enhanced AAV-mediated retinal transduction by ECVM following intravitreal administration. A previous study showed that bFGF enhanced AAV-mediated gene transduction in the rat brain.[27] We compared the relative expression of bFGF in ECVM-treated and control mouse retinas at 1 hour and 24 hours after treatment. Eyes receiving ECVM application showed significantly higher bFGF mRNA expression compared with the control retinas ($P = 0.0067$, $n = 12$ for each group, Mann–Whitney U test; Fig. 4A) at 1 hour after ECVM treatment. However, no significant difference of bFGF expression remained by 24 hours after ECVM. These results indicate that ECVM application transiently upregulates bFGF neurotrophin expression from Müller glial cells.

Müller glial reactivity/gliosis is implicated in improving AAV retinal transduction in the degenerating rat retina.[28] We examined Müller reactivity in mouse retinas that were treated by ECVM at 1 hour, 1 day, and 7 days after treatment, using a glial marker for Müller glial activation, the intermediate filament protein GFAP. The GFAP is normally expressed in astrocytes, but only expressed in Müller glia in stress. In control retinas, Müller cells did not express GFAP at any of the three time points (Fig. 4B, Control and not shown). However, anti-GFAP staining slightly increased in the Müller cells of ECVM-treated mouse retinas at 7 days (see Fig. 4B; ECVM - day 7), but not at 1 hour and 1 day after ECVM application (see Fig. 4B; ECVM - hour 1 and ECVM - day 1), indicating mild GFAP (+) Müller cell activation.

Because Müller glia endfeet are part of the ILM,[29] we performed further experiments to examine possible ILM structural changes after ECVM application. We co-stained vimentin, a well-known cytoskeleton marker for the intermediate filaments in Müller cells, and GFAP in retinal flat-mounts after ECVM at different time points (Fig. 4C). Compared with the control (see Fig. 4C-b), vimentin staining showed extensive changes in the cytoskeleton of Müller cell endfeet after ECVM treatment at days 1 and 2 (see Fig. 4C-e, h), indicating migration of Müller glia endfeet into the ILM. This vimentin staining pattern began to visibly

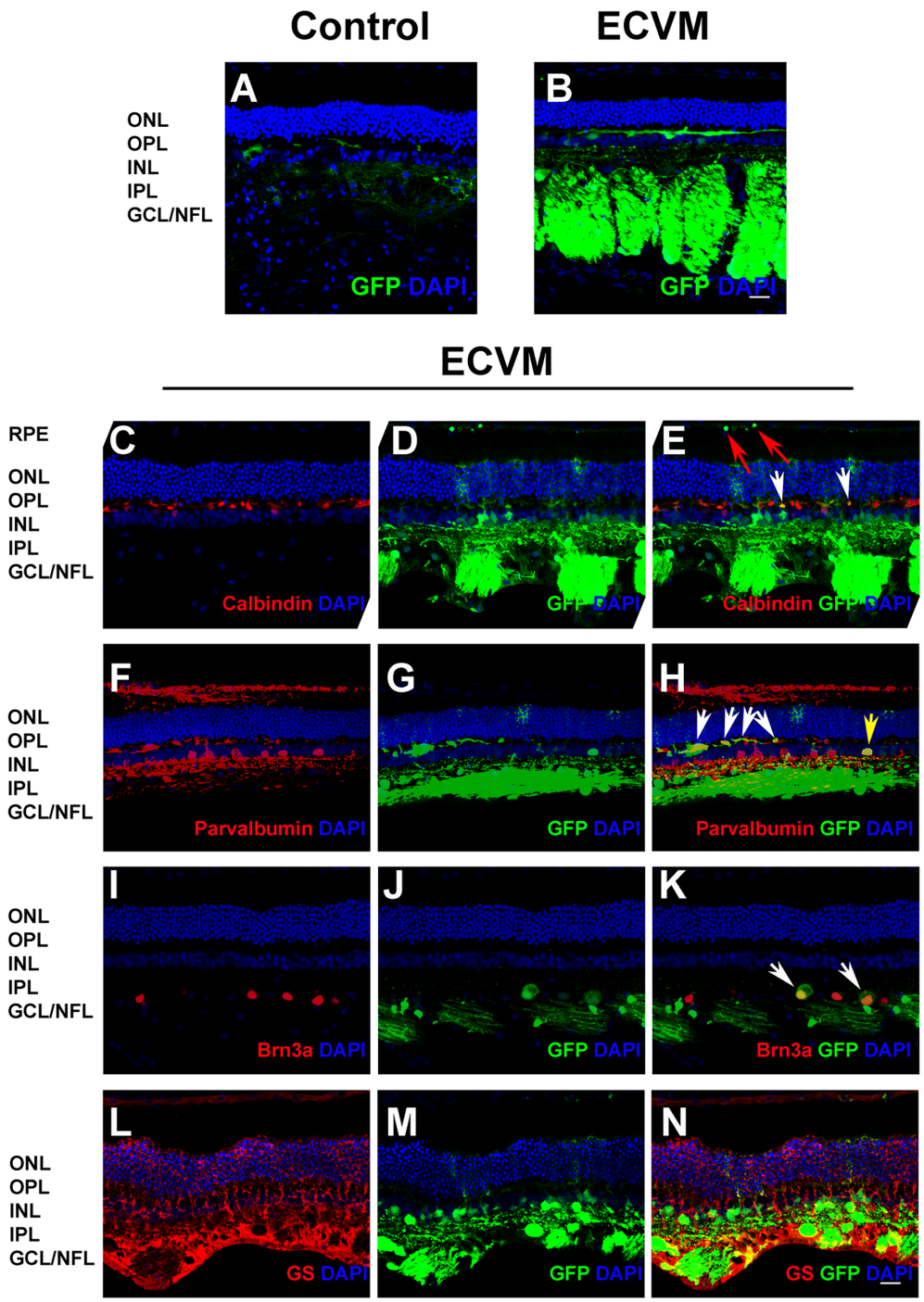

Figure 2. AAV8-GFP vectors penetrate and transduce deeper retina layers with ECVM application compared to eyes without current. Rabbit eyes were AAV8-GFP-injected (5×10^{11} vg/eye) with ECVM and collected 12 weeks post-injection. Vector-injected eyes without applying ECVM served as controls. (**A, B**) The representative images of the un-immunostained retinal sections of vector-injected control (Control, **A**) and vector-injected ECVM-treated eyes (ECVM, **B**) illustrate distribution of transduced cells in the retina, showing original GFP fluorescence in the inner retinal layers and the nerve fiber layer (NFL) in vector-injected ECVM-treated retina. *Scale bar:* 20 µm. (**C–N**) GFP-positive retinal sections of vector-injected ECVM-treated eyes were immunostained with antibodies against cell specific markers. Individual (original GFP fluorescence and different cell marker immunostaining) and merged images are shown, indicating that AAV vectors mediated GFP transduction in various cell types in ECVM-treated retinas. Images **C–N** are processed using Photoshop for a clearer view of the antibody staining. **C–E** Calbindin-positive horizontal cells (*white arrows*), GFP positive RPE cells (*red arrows*); **F–H** Parvalbumin-positive horizontal cells (*white arrows*) and parvalbumin-positive amacrine cells (*yellow arrow*); **I–K** Brn3a-positive ganglion cells (*white arrows*); **L–N** GS-positive Müller glial cells. RPE, retinal pigment epithelium; ONL, outer nuclear layer; OPL, outer plexiform layer; INL, inner nuclear layer; IPL, inner plexiform layer; GCL/NFL, ganglion cell layer/nerve fiber layer. *Scale bar*: 20 µm.

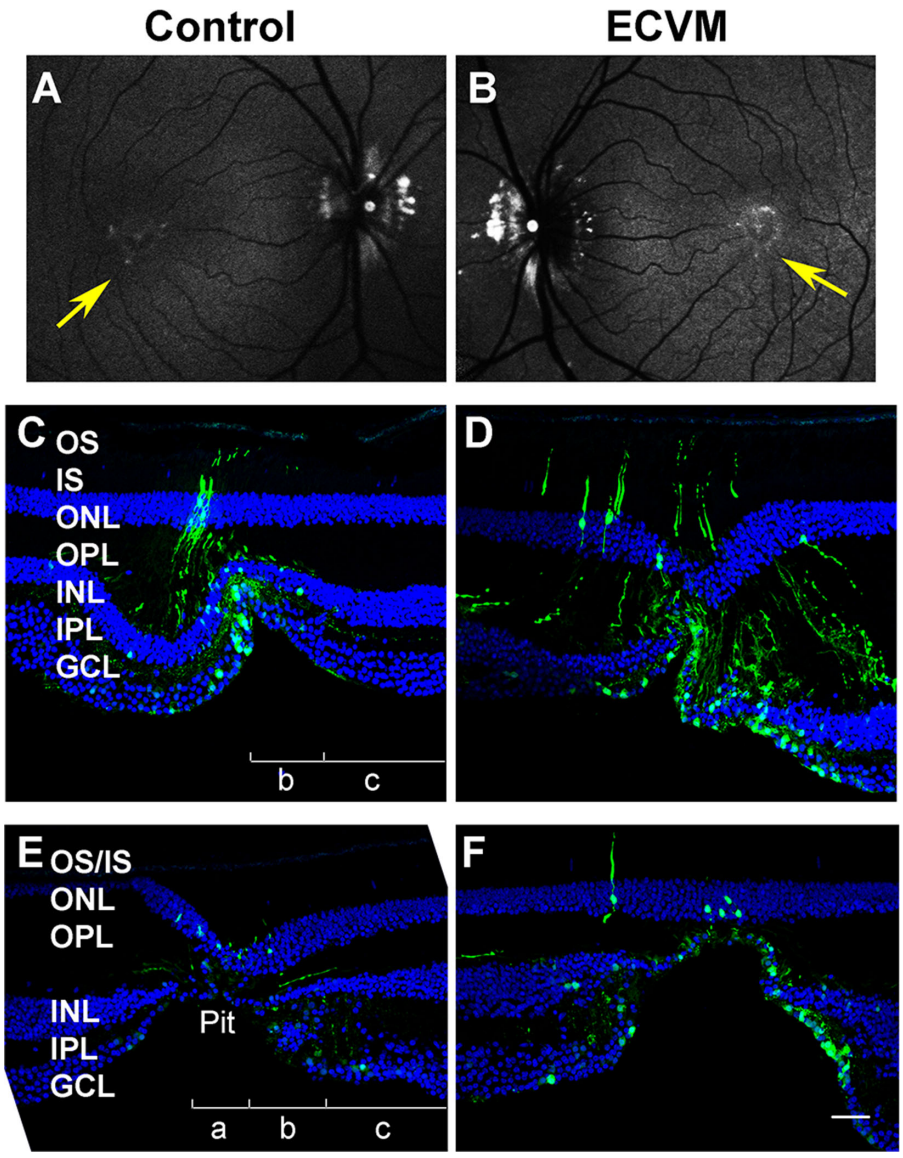

Figure 3. **ECVM promotes transduction of AAV8-GFP vectors in nonhuman primate retina after vitreous administration.** One eye of the rhesus macaque was treated with ECVM (continuous direct current, 850 µA/20 minutes) immediately after intravitreal delivery of AAV8-CMV-EGFP (1×10^{12} vg/eye). The other vector-injected eye without ECVM application served as control. Fundus images were taken at 12 weeks post-injection (PI). (**A, B**) Fundus images of injected eyes with (ECVM, **B**) and without electric current (Control, **A**) were shown. Compared with the control, GFP fluorescence signals were brighter in the foveal region (*yellow arrow*) of the injected-ECVM treated retina. (**C–F**) Representative images of retinal sections of vector injected-ECVM treated **D, F** and control **C, E** eyes illustrate distribution of transduced cells in the foveal regions, showing more GFP fluorescence throughout the retinal layers (from ganglion cells to photoreceptor cells) in vector-injected ECVM-treated retina. Compared with the areas shown in **C** and **D**, the images in **E** and **F** represented the areas closer to the central fovea (pit or foveola). a – Foveola, b – Fovea, c – Parafovea. OS, outer segment; IS, inner segment; ONL, outer nuclear layer; OPL, outer plexiform layer; INL, inner nuclear layer; IPL, inner plexiform layer; GCL, ganglion cell layer. *Scale bar*: 50 µm.

recover on day 4 (not shown) and day 7 (see Fig. 4C-k), suggesting that the cytoskeleton changes in Müller glia and ILM structural changes were transient. On the other hand, we were not able to detect reliable changes in GFAP expression in Müller glia on retinal flat-mounts at different time points observed (see Fig. 4C-d, g, j). Strong GFAP expression in normal astrocytes could obscure a slight increase in GFAP expression in Müller cells on retinal flat-mounts at day 7 as seen in retinal cross sections (see Fig. 4B; ECVM - day 7), suggesting minimal Müller cell gliosis after ECVM treatment.

These results indicate that transocular electric current modulates properties of Müller cells (i.e.

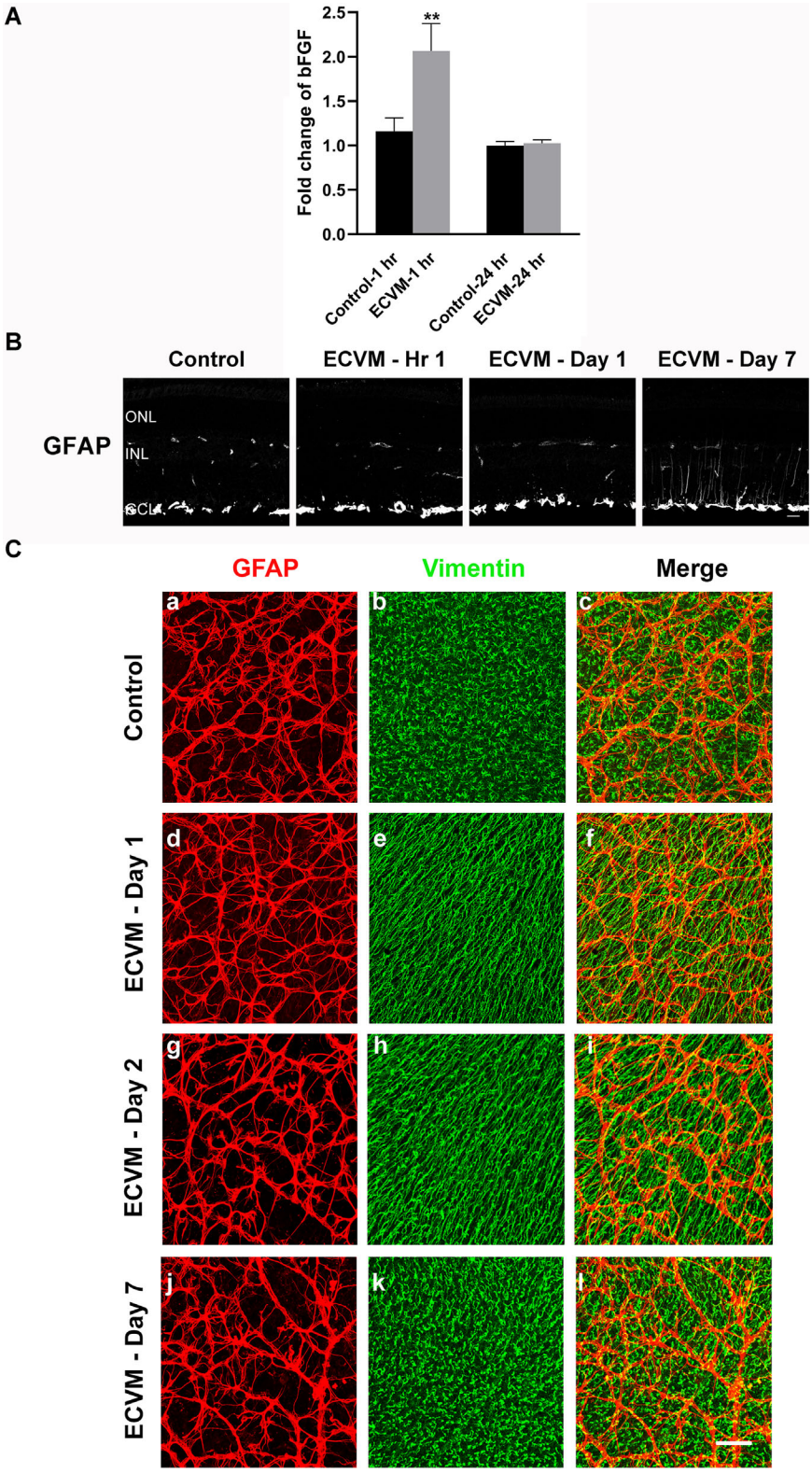

Figure 4. ECVM induces transient bFGF increase and mild Müller glial reactivity, and leads to ILM structural changes in mouse retina. WT mouse eyes were treated with ECVM (continuous, cornea negative, direct current, 10 µA/20 minutes). Untreated eyes served as controls. (**A**) For RT-PCR analysis of bFGF, retinal tissues were collected at 1 hour (Control - 1 hr, $n = 12$; ECVM - 1 hr, $n = 10$) and 24 hours (Control - 24 h, $n = 12$; ECVM - 24 h, $n = 9$) after treatment. Quantitative RT-PCR data are represented as a fold change in relative levels of bFGF expression compared to those in untreated WT control retinas. Expression of bFGF mRNA significantly increased at 1 hour after ECVM treatment (** $P = 0.0067$, Mann–Whitney U test). No significant changes of bFGF gene expression were detected in retinas between →

←
ECVM and control groups at 24 hours after treatment. (**B**) For analysis of Müller glial reactivity, mouse eyes were enucleated at 1 hour, 1 day, and 7 days after ECVM application. Retinal cross sections were immunostained with the anti-GFAP antibody. Representative images of GFAP-immunostained retinal sections of vector injected-ECVM treated eyes harvested at three time points (ECVM - hr 1, ECVM - day 1, and ECVM - day 7) after treatment and controls (Control) were shown, indicating occurrence of GFAP signals in Müller cells in the ECVM group only by 7 days after ECVM treatment. ONL, outer nuclear layer; INL, inner nuclear layer; GCL, ganglion cell layer. *Scale bar*: 20 µm. (**C**) For assessment of ILM organization in mouse retina after ECVM, mouse eyes were enucleated at day 1, 2, and 7 after ECVM application. Retinal flat-mounts were co-immunostained with the anti-GFAP and anti-vimentin antibodies. Representative confocal z-stack images of retinal flat-mounts from day 1 to day 7 after ECVM treatment were shown. Depth projections of vimentin staining show cytoskeleton changes in the endfeet of Müller glia in the ILM after ECVM most prominent at day 1 and 2 (e, h) and less persistent at day 7 (k). Temporal analysis of GFAP staining on retinal flat-mounts reveals minimal GFAP expression in Müller cells, suggesting minimal Müller gliosis after ECVM treatment. *Scale bar*: 50 µm.

bFGF neurotrophin expression and glial reactivity) and leads to ILM structural changes, which may contribute to enhanced AAV-mediated gene transduction in the retina by transocular ECVM. We also infer that Müller cell activation in the X-linked retinoschisis (XLRS) retina may underlie the increased AAV vector uptake we constantly observed in the RS1 KO mouse.[23,30,31]

Discussion

These data provide evidence that transocular ECVM promotes the transduction efficiency of AAV8-CMV-GFP in normal rabbit and monkey retinas following intravitreal injection. In addition to the mouse retina shown previously,[9] this study demonstrates the utility of the ECVM technique to enhance penetration and expression of an AAV-vector construct into the retina of two other species, the rabbit and macaque, following administration into the vitreous. Although the ECVM effects were less in rabbit and NHP than we observed in wild type mouse, the present data were the first proof-of-concept that a similar process may be involved in the larger eyes of these species. We propose that the ECVM effect needs further exploration of electric current magnitude, duration, and pulse modulation to enhance the effects we observed in this study.

The transduced regions in the rabbit and monkey retinas were relatively smaller and less penetrative than we had seen for the ECVM method in wild type mice. However, it is important to recognize that the eyes of the mouse and large animals (e.g. the rabbit and monkey) are quite different in the dimensions of the posterior surface of the lens relative to the retinal ILM surface. We have made no effort yet to optimize the electrical current nor the vector administration into the vitreous cavities in these experiments. More importantly, this work illustrates that the approach of combining ECVM with intravitreal administration may be useful to augment retinal penetration and transduction of AAV vectors in large-animal models, as an essential step forward toward the clinical development of this strategy.

The AAV vector must traverse multiple vitreous, ILM, and retinal barriers to effectively transduce retinal cells after intravitreal administration. The vitreous humor is the first barrier. This is a gel-like material that fills the posterior segment cavity. Electric fields may enhance AAV mobility in the vitreous by electrorepulsion from the electrode.[32,33] The AAV virus carries a net negative charge in the vitreous (pH 7.4–7.52)[34] and applying negative voltage at the cornea might enhance AAV vector diffusion toward the ILM. This study extends our previous ECVM work to the rabbit and monkey. Compared to wild type mice,[9] the rabbit and monkey had relative smaller retinal areas and/or fewer outer retinal cells transduced by AAV vectors with ECVM. One possible factor for this is that the large size of the eyeball and vitreous (the axial length and volume) may limit AAV viral particles from reaching the retina, particularly photoreceptors and RPE. In future studies, we can deliver viral particles in the posterior vitreous cavity closer to the retina of the large animals to reduce the distance through the vitreous, and test whether this would further increase the efficiency of AAV-mediated retinal transduction by ECVM.

Our results suggest a further possible mechanism by which transocular ECVM enhances the transduction efficiency in normal retina. In mouse, RT-PCR data (see Fig. 4A) showed that expression of basic fibroblast growth factor (bFGF) increased significantly by 1 hour after ECVM treatment with 10 µA current. This finding is consistent with other previous studies, for example, whole-eye electrical stimulation at 4 µA in vivo upregulated bFGF in Müller cells and was neuroprotective against retinal degeneration in P23H-1 rats.[35] The bFGF is known to enhance transduction, distribution, and transport of AAV vectors in the rat brain.[27] In the rat brain, co-injection of bFGF along with the AAV2 vector resulted in enhanced AAV-mediated gene delivery and transduction, possibly by

competing with AAV2 interaction with their receptors and then blocking AAV2-binding sites. Inhibition of AAV2 entry sites would allow AAV particles to diffuse farther through the brain tissue before transduction occurs and thereby extending AAV distribution within rat striatum. It is worth noting that the positive effect of bFGF on AAV2 distribution in this study is independent of AAV2-FGFR1 interaction, because the striatum does not express FGFR1,[36] a co-receptor for AAV2 vector.[37] This finding indicates that the effect of bFGF on AAV distribution might not be AAV serotype dependent. It is possible that Müller glial cells upregulate bFGF neurotrophin expression in response to retinal stress (i.e. transocular ECVM) and, in turn, this may enhance AAV-mediated gene delivery and transduction within retinal tissues. It warrants consideration that increasing exogenous bFGF in the retina may act as an adjuvant for retinal distribution and transduction of AAV vectors.

In our study with 10 µA current, we found that the bFGF upregulation by ECVM was transient and returned to normal by 24 hours after current application, indicating that effects from a single ECVM treatment are relatively short lived. Repeating ECVM application (e.g. daily or 3 times/week, etc.) may further improve the transduction efficiency of AAV vectors.

We also found that transocular ECVM induced a slight increase of the intermediate filament protein GFAP expression in Müller cells and led to transient cytoskeleton changes of Müller glia endfeet in the retina. The ILM is the basement membrane formed by the endfeet of the Müller cells[29] and is an important barrier for AAV retinal transduction from the vitreous.[17] Further, Müller cell processes at the ILM showed structural alteration at the endfeet, in the pattern of vimentin staining of cytoskeleton intermediate filaments, immediately after ECVM treatment and lasting for several days. As the radial morphology of Müller cells spans the retinal layers, these ILM structural changes may allow AAV access for deeper penetration and transduction. This idea is supported by the previous study that ILM structural changes in the degenerating rat retina are implicated in improving AAV retinal transduction from the vitreous.[28] In our study, AAV transduction and expression were observed in Müller cells, including processes stretching across the entire retina (see Figs. 2L–2N).

In conclusion, we have found evidence that ECVM may be useful to enhance transduction of AAV vectors by intravitreal injection in large-animal eyes. It warrants further studies to optimize this approach, to refine the ECVM parameters, and by manipulating the technique for intravitreal injection.

Acknowledgments

The authors thank Jinbo Li and Maria Santos for technical assistance; Ginger Tansey and supporting staff at the Building 49 Central Animal Facility (NEI, NIH) for animal support.

Supported by the National Institutes of Health Intramural Research Programs of the National Institute on Deafness and Other Communication Disorders and the National Eye Institute.

Disclosure: **H. Song**, None; **Y. Zeng**, None; **S.P.B. Sardar Pasha**, None; **R.A. Bush**, None; **C. Vijayasarathy**, None; **H. Qian**, None; **L. Wei**, None; **H.E. Wiley**, None; **Z. Wu**, None; **P.A. Sieving**, None

References

1. Rodrigues GA, Shalaev E, Karami TK, Cunningham J, Slater NKH, Rivers HM. Pharmaceutical development of AAV-based gene therapy products for the eye. *Pharm Res*. 2018;36:29.
2. Carvalho LS, Vandenberghe LH. Promising and delivering gene therapies for vision loss. *Vision Res*. 2015;111:124–133.
3. Ali RR, Reichel MB, De Alwis M, et al. Adeno-associated virus gene transfer to mouse retina. *Hum Gene Ther*. 1998;9:81–86.
4. Auricchio A, Kobinger G, Anand V, et al. Exchange of surface proteins impacts on viral vector cellular specificity and transduction characteristics: the retina as a model. *Hum Mol Genet*. 2001;10:3075–3081.
5. Lebherz C, Maguire A, Tang W, Bennett J, Wilson JM. Novel AAV serotypes for improved ocular gene transfer. *J Gene Med*. 2008;10:375–382.
6. Natkunarajah M, Trittibach P, McIntosh J, et al. Assessment of ocular transduction using single-stranded and self-complementary recombinant adeno-associated virus serotype 2/8. *Gene Ther*. 2008;15:463–467.
7. Igarashi T, Miyake K, Asakawa N, Miyake N, Shimada T, Takahashi H. Direct comparison of administration routes for AAV8-mediated ocular gene therapy. *Curr Eye Res*.2013;38:569–577.
8. Hellstrom M, Ruitenberg MJ, Pollett MA, Ehlert EM, Twisk J, Verhaagen J, et al. Cellular tropism and transduction properties of seven adeno-associated viral vector serotypes in adult

retina after intravitreal injection. *Gene Ther*. 2009;16:521–532.
9. Song H, Bush RA, Zeng Y, Qian H, Wu Z, Sieving PA. Trans-ocular electric current in vivo enhances AAV-mediated retinal gene transduction after intravitreal vector administration. *Mol Ther Methods Clin Dev*. 2019;13:77–85.
10. Hughes A. A schematic eye for the rabbit. *Vision Res*. 1972;12:123–138.
11. Lapuerta P, Schein SJ. A four-surface schematic eye of macaque monkey obtained by an optical method. *Vision Res*. 1995;35:2245–2254.
12. Deering MF. A photon accurate model of the human eye. *ACM Trans Graph*. 2005;24:649–658.
13. Gwon A. The Rabbit in Cataract/IOL Surgery, in Animal Models in Eye Research, Tsonis PA, eds. San Diego, CA: Academic Press; 2008: 184–204.
14. Gwon A. The Primate in Cataract/IOL Surgery, in Animal Models in Eye Research, Tsonis PA, eds. San Diego, CA: Academic Press; 2008: 205–208.
15. Atsumi I, Kurata M, Sakaki H. Comparative study on ocular anatomical features among rabbits, beagle dogs and cynomolgus monkeys. *Anim. Eye Res*. 2013;32:35–41.
16. Ahn SJ, Hong HK, Na YM, et al. Use of rabbit eyes in pharmacokinetic studies of intraocular drugs. *J Vis Exp*. 2016;113;53878.
17. Dalkara D, Kolstad KD, Caporale N, et al. Inner limiting membrane barriers to AAV-mediated retinal transduction from the vitreous. *Mol Ther*. 2009;17:2096–2102.
18. Schultz BR, Chamberlain JS. Recombinant adeno-associated virus transduction and integration. *Mol Ther*. 2008;16:1189–1199.
19. Kotterman MA, Yin L, Strazzeri JM, Flannery JG, Merigan WH, Schaffer DV. Antibody neutralization poses a barrier to intravitreal adeno-associated viral vector gene delivery to non-human primates. *Gene Ther*. 2015;22:116–126.
20. Heier JS, Kherani S, Desai S, et al. Intravitreous injection of AAV2-sFLT01 in patients with advanced neovascular age-related macular degeneration: a phase 1, open-label trial. *Lancet*. 2017;390:50–61.
21. Boutin S, Monteilhet V, Veron P, et al. Prevalence of serum IgG and neutralizing factors against adeno-associated virus (AAV) types 1, 2, 5, 6, 8, and 9 in the healthy population: implications for gene therapy using AAV vectors. *Hum Gene Ther*. 2010;21:704–712.
22. Lee S, Kang IK, Kim JH, et al. Relationship between neutralizing antibodies against adeno-associated virus in the vitreous and serum: effects on retinal gene therapy. *Transl Vis Sci Technol*. 2019;8:14.
23. Park TK, Wu Z, Kjellstrom S, et al. Intravitreal delivery of AAV8 retinoschisin results in cell type-specific gene expression and retinal rescue in the Rs1-KO mouse. *Gene Ther*. 2009;16:916–926.
24. Marangoni D, Bush RA, Zeng Y, et al. Ocular and systemic safety of a recombinant AAV8 vector for X-linked retinoschisis gene therapy: GLP studies in rabbits and Rs1-KO mice. *Mol Ther Methods Clin Dev*. 2016;5:16011.
25. Song H, Vijayasarathy C, Zeng Y, et al. NADPH oxidase contributes to photoreceptor degeneration in constitutively active RAC1 mice. *Invest Ophthalmol Vis Sci*. 2016;57:2864–2875.
26. Sardar Pasha SPB, Munch R, Schafer P, et al. Retinal cell death dependent reactive proliferative gliosis in the mouse retina. *Sci Rep*. 2017;7:9517.
27. Hadaczek P, Mirek H, Bringas J, Cunningham J, Bankiewicz K. Basic fibroblast growth factor enhances transduction, distribution, and axonal transport of adeno-associated virus type 2 vector in rat brain. *Hum Gene Ther*. 2004;15:469–479.
28. Kolstad KD, Dalkara D, Guerin K, et al. Changes in adeno-associated virus-mediated gene delivery in retinal degeneration. *Hum Gene Ther*. 2010;21:571–578.
29. Candiello J, Balasubramani M, Schreiber EM, et al. Biomechanical properties of native basement membranes. *FEBS J*. 2007;274:2897–2908.
30. Takada Y, Vijayasarathy C, Zeng Y, Kjellstrom S, Bush RA, Sieving PA. Synaptic pathology in retinoschisis knockout (Rs1-/y) mouse retina and modification by rAAV-Rs1 gene delivery. *Invest Ophthalmol Vis Sci*. 2008;49:3677–3686.
31. Bush RA, Zeng Y, Colosi P, et al. Preclinical dose-escalation study of intravitreal AAV-RS1 gene therapy in a mouse model of X-linked retinoschisis: dose-dependent expression and improved retinal structure and function. *Hum Gene Ther*. 2016;27:376–389.
32. Guy RH, Kalia YN, Delgado-Charro MB, Merino V, Lopez A, Marro D. Iontophoresis: electrorepulsion and electroosmosis. *J Control Release*. 2000;64:129–132.
33. Li SK, Jeong EK, Hastings MS. Magnetic resonance imaging study of current and ion delivery into the eye during transscleral and transcorneal iontophoresis. *Invest Ophthalmol Vis Sci*. 2004;45:1224–1231.
34. Chirila TV, Hong Y. The vitreous humor, in Handbook of Biomaterial Properties, Second edition, Murphy JBW, Hastings G, Eds. New York: Springer; 2016:127.

35. Hanif AM, Kim MK, Thomas JG, et al. Whole-eye electrical stimulation therapy preserves visual function and structure in P23H-1 rats. *Exp Eye Res*. 2016;149:75–83.
36. Belluardo N, Wu G, Mudo G, Hansson AC, Pettersson R, Fuxe K. Comparative localization of fibroblast growth factor receptor-1, -2, and -3 mRNAs in the rat brain: in situ hybridization analysis. *J Comp Neurol*. 1997;379:226–246.
37. Qing K, Mah C, Hansen J, Zhou S, Dwarki V, Srivastava A. Human fibroblast growth factor receptor 1 is a co-receptor for infection by adeno-associated virus 2. *Nat Med*. 1999;5:71–77.